Hindawi Publishing Corporation
Active and Passive Electronic Components
Volume 2007, Article ID 40249, 8 pages
doi:10.1155/2007/40249

Review Article

Resonant Excitation of Terahertz Surface Plasmons in Subwavelength Metal Holes

Weili Zhang,[1] Abul K. Azad,[1,2] and Jiaguang Han[1,3]

[1] *School of Electrical and Computer Engineering, Oklahoma State University, Stillwater, OK 74078-5032, USA*
[2] *MPA-CINT, Los Alamos National Laboratory, P. O. Box 1663, MS K771, Los Alamos, NM 87545, USA*
[3] *Department of Physics, National University of Singapore, 2 Science Drive 3, Singapore 117542*

Received 27 September 2007; Accepted 12 October 2007

Recommended by Yalin Lu

We present a review of experimental studies of resonant excitation of terahertz surface plasmons in two-dimensional arrays of subwavelength metal holes. Resonant transmission efficiency higher than unity was recently achieved when normalized to the area occupied by the holes. The effects of hole shape, hole dimensions, dielectric function of metals, polarization dependence, and array film thickness on resonant terahertz transmission in metal arrays were investigated by the state-of-the-art terahertz time-domain spectroscopy. In particular, extraordinary terahertz transmission was demonstrated in arrays of subwavelength holes made even from Pb, a generally poor metal, and having thickness of only one-third of skin depth. Terahertz surface plasmons have potential applications in terahertz imaging, biosensing, interconnects, and development of integrated plasmonic components for terahertz generation and detection.

1. INTRODUCTION

Recent advance in extraordinary transmission of light has shown that the fascinating properties of two-dimensional (2D) plasmonic arrays of subwavelength holes could lead to breakthrough applications in photonics, nanofabrication, and biochemical sensing. It thus has stimulated extensive research interest in a broad spectral region, in particular, at terahertz frequencies [1–15]. Surface plasmons (SPs) are collective excitations for quantized oscillations of electrons. The resonant interaction between electron-charged oscillations near the surface of metal and the electromagnetic field creates SPs and results in rather unique properties [16]. It was demonstrated that when light passed through periodic subwavelength holes perforated in a metallic film, the observed extraordinary transmission was attributed to resonant excitation of SPs [1, 17]. Light was coupled into the holes in the form of SPs which were squeezed through the holes and then converted back into light on the far side of the holes. Extensive experimental and theoretical studies have been carried out to approach fundamental understanding of this extraordinary transmission and to explore its potential applications in a broad range of disciplines [18–21].

In the terahertz regime, SPs have recently attracted much attention and become an emerging new area [4–15, 22, 23]. SP-enhanced terahertz transmission was observed in subwavelength hole arrays patterned on both metallic films and doped semiconductor slabs. In this article, a review of experimental studies on resonant terahertz transmission in lithographically fabricated 2D metallic arrays of subwavelength holes is presented. Enhanced terahertz transmission in both optically thick and optically thin metallic arrays was experimentally demonstrated. At the primary SP $[\pm 1,0]$ mode, amplitude transmission efficiency of up to nine tenths of the maximum resonant transmission was achieved when a film thickness was only one third of the skin depth [14]. By use of highly reproducible subwavelength arrays, we have demonstrated the effect of dielectric function of metals on transmission properties of terahertz radiation [15]. Additionally, we showed that the enhanced terahertz transmission in the 2D arrays of subwavelength holes resulted from contributions of both SPs and nonresonant transmission [22].

2. TERAHERTZ SPs IN METAL ARRAYS

At terahertz frequencies, a drastic increase in the value of dielectric constant $\varepsilon_m = \varepsilon_{\mathrm{rm}} + i\varepsilon_{\mathrm{im}}$ has made most metals

become highly conductive. This has resulted in discrepancies in SP-enhanced terahertz transmission with that in the visible spectral region. Experimental results on transmission properties of light in metallic structures indicated that SP-enhanced transmission is normally achieved in metals with large ratio of the real to the imaginary dielectric constant, $-\varepsilon_{\mathrm{rm}}/\varepsilon_{\mathrm{im}} \gg 1$ [24, 25]. In the terahertz regime, however, this ratio becomes $-\varepsilon_{\mathrm{rm}}/\varepsilon_{\mathrm{im}} < 1$ for nontransition metals such as Ag, Au, Cu, and Al [26]. This was considered as a limitation to realize resonant excitation of terahertz SPs in the 2D hole arrays. A recent theoretical work, however, has shown that an appropriate surface corrugation gives rise to an effective dielectric constant and facilitates the establishment of SPs, even with $-\varepsilon_{\mathrm{rm}}/\varepsilon_{\mathrm{im}} < 1$ [27]. Extraordinary terahertz transmission was observed in subwavelength hole arrays made from both good and poor electrical conductors [15].

2.1. Resonant excitation of terahertz SPs in optically thick metal arrays

Resonant transmission of terahertz pulses in optically thick metallic films patterned with subwavelength hole arrays was experimentally demonstrated in a broad terahertz spectral range [4]. Terahertz time-domain spectroscopy (THz-TDS) measurements have revealed enhanced amplitude transmission and a sharp phase peak centered at the SP [±1,0] resonance mode. It was also found that the aperture shape has a remarkable effect on the transmission properties of the 2D hole arrays. Figures 1(a) and 1(b) illustrate the transmitted terahertz pulses and the corresponding amplitude spectra of the reference and the samples. The arrays were lithographically fabricated with 520-nm-thick aluminum film deposited on silicon substrate. Sample A is a square array of 80 μm (x axis) × 100 μm (y axis) rectangular holes as shown in the inset of Figure 1(a), while sample B is a square array of 100-μm-diameter circular holes. The period of these arrays is L = 160 μm in both 2D directions. The THz-TDS transmission measurements were performed with linearly polarized terahertz ($E//x$) waves impinging on the array at normal incidence [4].

The amplitude transmission and the corresponding phase change are shown in Figures 2(a) and 2(b), respectively. The transmission is obtained from the ratio between the Fourier-transformed sample and the reference amplitudes, whereas the phase change is the phase difference between the sample and the reference spectra. At terahertz frequencies, the dielectric constant of metals is several orders higher than that of dielectric media. Here, $\varepsilon_m = -3.4 \times 10^4 + 1.3 \times 10^6 i$ for aluminum, while $\varepsilon_d = 11.68$ and $\varepsilon_d = 1$ for silicon and air, respectively. Thus the SP modes excited in the array can be approximately given as [4, 28]

$$\omega_{\mathrm{SP}}^{m,n} \cong cG_{mn}\varepsilon_d^{-1/2}, \tag{1}$$

where $G_{mn} = (2\pi/L)(m^2 + n^2)^{1/2}$ is the grating momentum wave vector for 2D square hole arrays, L is the lattice constant of the array, c is the speed of light in vacuum, and m and n are integers of the SP modes. The observed sharp phase peaks centered at the SP resonance modes are indicated by the vertical dashed lines: the metal-Si modes at 0.548 [±1,0] and 0.775 [±1,±1] THz; the metal-air mode [±1,0] at 1.875 THz. Besides samples A and B, a set of arrays with rectangular, square, and circular holes has been measured. We observed that, with the same fundamental period, the hole shape and dimensions can appreciably modify the strengths and shapes of the transmission and the phase change peaks due to the polarization dependent coupling of SPs.

2.2. SP-enhanced terahertz transmission in optically thin metallic arrays

So far, resonant excitation of SPs has been widely studied in optically thick 2D hole arrays in a broad spectral range. It is intriguing whether SPs can be excited in optically thin metallic arrays of sub-skin-depth thickness. Here, we demonstrate resonant terahertz transmission through subwavelength hole arrays patterned on metallic films with thicknesses less than a skin depth. Our experimental results have revealed a critical array thickness, above which the SP resonance occurs [14]. The maximum amplitude transmission was achieved when the thickness of metal film approaches a skin depth. However, enhanced terahertz transmission of up to nine tenths of the maximum transmission was realized at a film thickness of only one third of the skin depth at 0.55 THz. This finding may extensively reduce the metal thickness of plasmonic crystals for applications in photonics, optoelectronics, and sensors.

The metallic arrays made from Pb were lithographically fabricated on a silicon wafer (0.64 mm thick p-type resistivity ρ = 20 Ωcm) as shown in the inset of Figure 1(a) [4]. The rectangular holes have physical dimensions of 100 μm × 80 μm with a lattice constant of 160 μm. Pb was chosen as the constituent metal of the arrays mainly because of two reasons. First, the extraordinary terahertz transmission in Pb subwavelength hole arrays has been demonstrated with an amplitude efficiency of up to 82% at 0.55 THz, which is close to the performance of arrays made from good electrical conductors such as Ag, Al, and Au [15]. Second, the skin depth of Pb at 0.55 THz is 320 nm, nearly three times of those of Ag and Al. It thus provides a large dynamic range to characterize the evolution of SP resonance at subskin-depth thickness.

The value of skin depth of electromagnetic waves in metal is determined by the penetration distance at which the electric field falls to 1/e. The SPs, which propagate on metal-dielectric interface, decay exponentially in both media. At terahertz frequencies, the complex wave vector inside the metal perpendicular to the interface is approximately given as $k_z = (\omega/c)\varepsilon_m^{1/2}$ [4, 14, 15], where ω is the angular frequency. Since only the imaginary part of k_z causes the exponential decay of electric fields, the skin depth is defined as $\delta = 1/\mathrm{Im}(k_z) = (c/\omega)\lfloor 1/\mathrm{Im}(\varepsilon_m^{1/2})\rfloor$. Based on this relation, the skin depths for Pb, Al, and Ag at 0.55 THz, the primary SP [±1, 0] resonance are estimated as 320, 110, and 83 nm, respectively.

Pb arrays with various thicknesses ranging from 60 to 1000 nm were prepared. In the THz-TDS measurements, the input terahertz pulses are polarized along the minor axes (80 μm) of the rectangular holes and penetrate the array at normal incidence. In Figure 3, evolution of SP resonance as

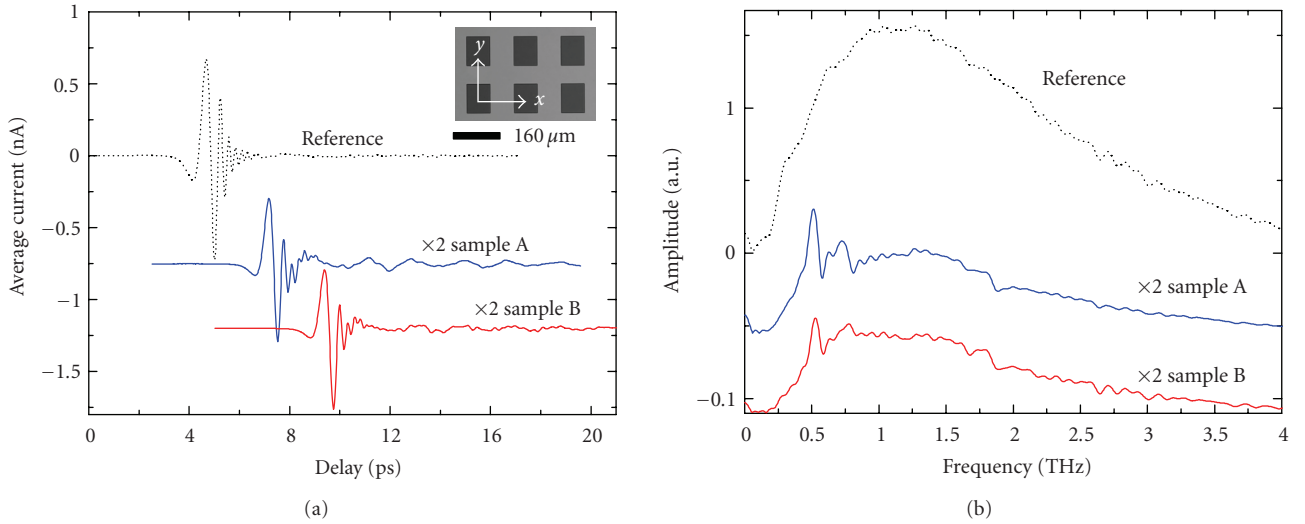

Figure 1: (a) THz-TDS measured transmitted terahertz pulses and (b) the corresponding spectra through the reference and array samples (multiplied by two). The curves in both (a) and (b) are displaced vertically for clarity. Inset: microscopic image of the array.

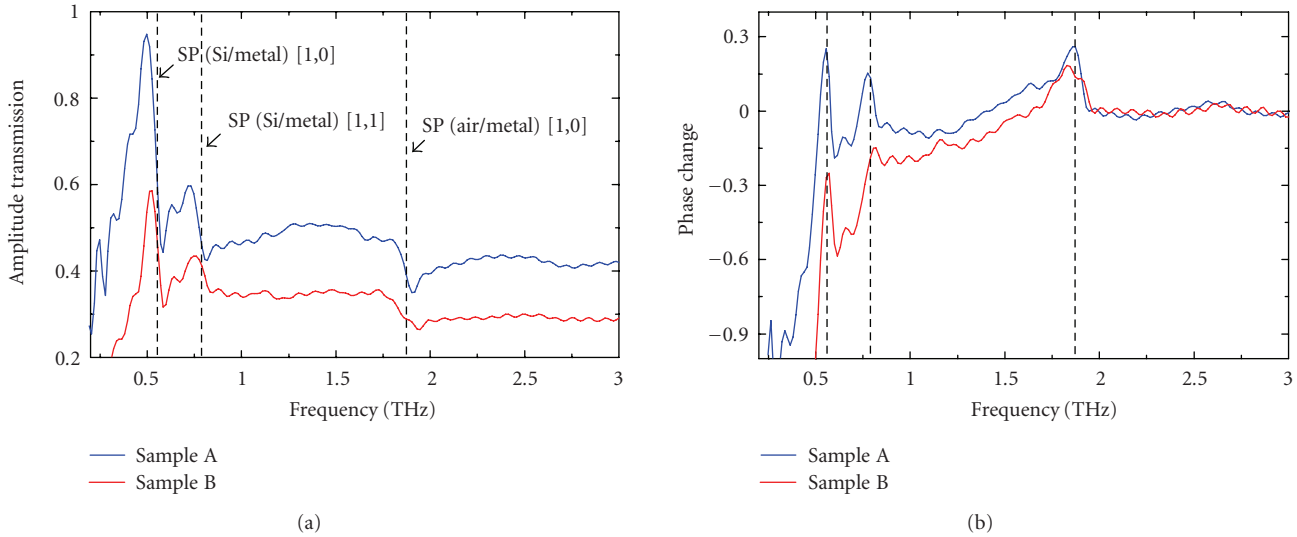

Figure 2: (a) Amplitude transmission of terahertz pulses through the array samples A and B. (b) Corresponding phase change in radians. The dashed lines indicate the SP resonant frequencies.

a function of array film thickness is depicted in the amplitude transmission spectra of various arrays. It clearly reveals two regions of thickness dependence. Below the critical thickness, 64 nm, the frequency-dependent transmission is nearly flat, showing no resonance peak. Above the critical thickness, a resonance at 0.55 THz appears in the transmission, whose amplitude increases with array thickness while the background transmission is reduced at the mean time. This resonance is attributed to the excitation of SPs at the Pb-Si interface. Immediately above the critical thickness, the resonance amplitude is very sensitive to the thickness of arrays. The dependence of peak transmission on array thickness above the critical thickness is shown in Figure 4. The amplitude transmission efficiency increases exponentially when the array thickness is below 100 nm. It then saturates gradually and approaches the maximum at one skin depth [14]. It is worth noting that a transmission efficiency as high as 76% was achieved at array thickness of 100 nm, only one third of skin depth. This value is more than nine tenths of the maximum transmission efficiency achieved at one skin depth. For comparison, we have fabricated two additional arrays of the same structure but made from Ag and Al of one third of skin depth. The measured transmission efficiencies are all above nine tenths of their maximum amplitude transmission.

2.3. *Effect of dielectric function of metals on terahertz SPs*

In the visible spectral region, the dielectric function of metals was demonstrated to play a crucial role in the extraordinary transmission in 2D subwavelength hole arrays. Because

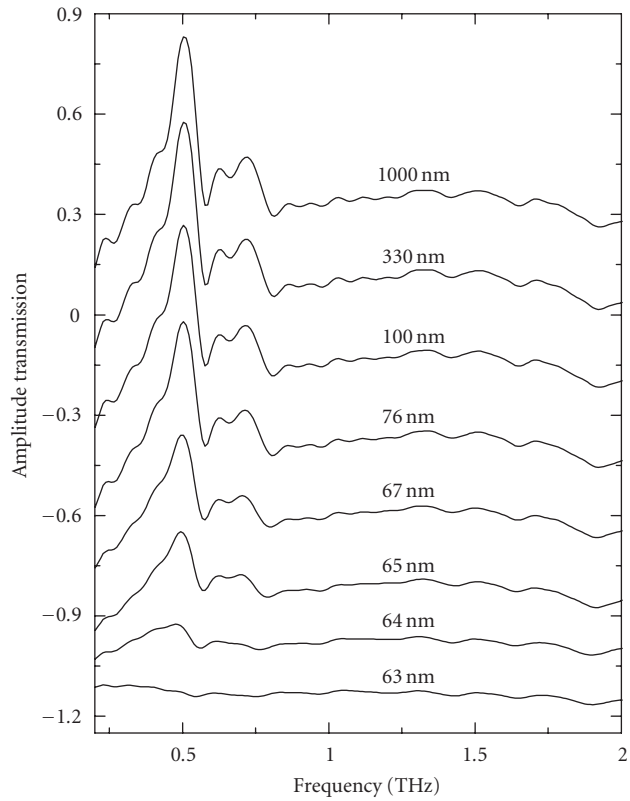

Figure 3: Amplitude transmission of terahertz pulses through the Pb arrays with different film thicknesses. The curves are vertically displaced for clarity.

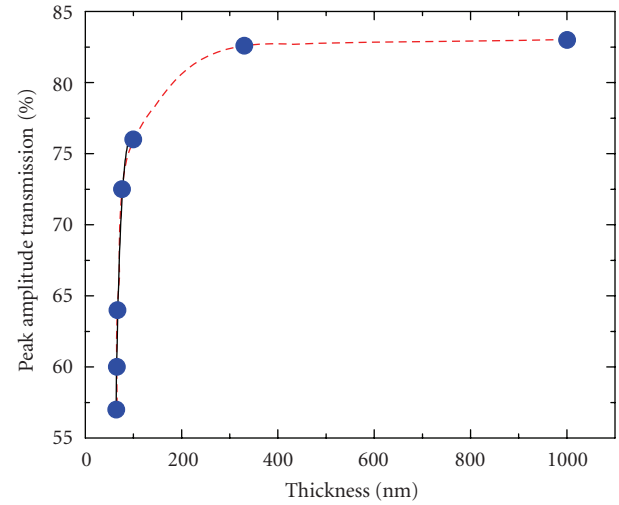

Figure 4: Peak amplitude transmission of the SP [±1,0] mode at 0.55 THz as a function of the Pb thickness (circles). The solid curve is an exponential fit to the data with array thickness below 100 nm. The dashed curve is a guide to the eye.

of a different ratio $-\varepsilon_{rm}/\varepsilon_{im}$, the transmission properties of light showed a large difference in arrays made from different metals [1, 24, 25]. The SP-enhanced transmission efficiency of light was increased with a higher ratio $-\varepsilon_{rm}/\varepsilon_{im}$ [24, 25]. At terahertz frequencies, however, the dielectric constant of metals is several orders of magnitude higher than that at visible frequencies. It is essential to explore how the dielectric function of metals influences extraordinary terahertz transmission in subwavelength structures.

Two types of metallic arrays were lithographically fabricated: array-on-silicon samples with patterned optically thick metal film on blank silicon substrate for the metal-silicon [±1,0] mode 0.55 THz [4, 15]; and freestanding metallic arrays for the metal-air [±1,0] mode 1.60 THz [10, 15]. At 0.55 THz, the ratios $-\varepsilon_{rm}/\varepsilon_{im}$ for Ag, Al, and Pb are 0.12, 0.03, and 0.01, respectively, which indicate that Ag is still a better metal than others and expected to show resonance with higher-amplitude transmission [25]. Realistically, the Ag array indeed shows the highest amplitude transmission 87%, while the Al and Pb arrays follow after with small attenuation, giving 85.5% and 82%, respectively. Even though the amplitude transmission of these arrays shows small difference, it indeed increases with higher ratio $-\varepsilon_{rm}/\varepsilon_{im}$. This result is consistent with those observed at visible frequencies [24, 25].

Compared to excellent metals, Pb is generally considered as a poor electrical conductor. However, the drastic increase in dielectric constant enables Pb to behave as a better metal towards the establishment of SP-enhanced transmission at terahertz frequencies. The measured peak transmissions at the SP [±1,0] resonance 1.60 THz for Ag, Al, and Pb are 82%, 81%, and 72.5%, respectively, showing similar properties as observed at the SP [±1,0] metal-Si resonance 0.55 THz. The difference in amplitude transmission for arrays made from these metals is arisen from the difference in effective propagation length of SPs.

Besides the metal arrays of skin-depth thickness, we have fabricated array-on-silicon samples with different thicknesses to verify the experimental results observed above. Figure 5 presents the peak transmittance measured at the 0.55 [±1,0] THz SP mode for the Ag, Al, and Pb arrays. With metal thicknesses of one-third and three times of skin-depth, the comparison of peak transmittance for different metals remains the same trend as observed with one skin-depth thickness, demonstrating the consistency of our measurements.

The difference in resonant transmission for arrays made from different metals is primarily arisen from the difference in effective propagation length of SPs, determined mainly by internal damping and radiation and scattering damping [3]. At terahertz frequencies, the imaginary propagation vector along the metal-dielectric interface, approximately given as $k_i = k_0\varepsilon_d^{3/2}/(2\varepsilon_{im})$ [4], governs the internal damping, where k_0 is the wave vector of electromagnetic wave in vacuum. Figure 6 shows the calculated k_i for SP resonances along both the metal-Si and the metal-air interfaces. The measured transmission of the metal arrays indeed decreases with increasing k_i. On a rough metal surface, besides the internal absorption, radiation and scattering damping also modify the propagation length [17]. As a result, the effective propagation lengths for different metals can be extensively reduced, leading to the difference in the resonant transmission.

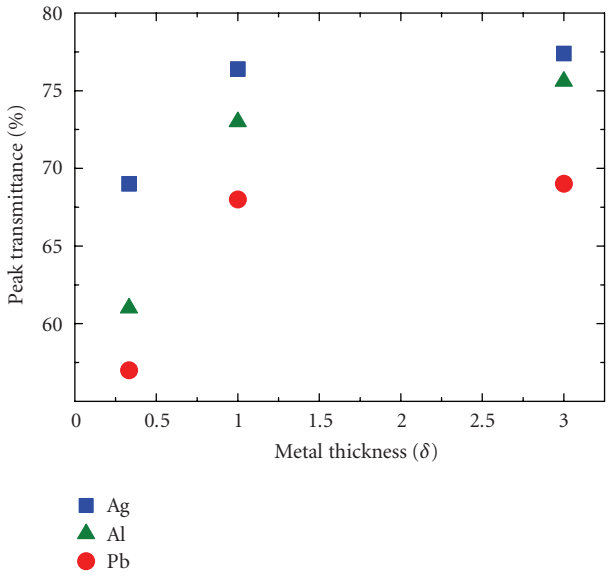

FIGURE 5: Peak transmittance at the 0.55 [±1,0] THz metal-Si mode for arrays made from Ag, Al, and Pb with different metal thicknesses. The arrays are metal on silicon with rectangular holes of dimensions 100 μm × 80 μm.

2.4. *Coupling between SPs and nonresonant transmission*

SPs excited at the surface of the 2D hole arrays were demonstrated to play a dominant role in extraordinary transmission of electromagnetic waves [1, 17]. The recent studies, however, have revealed that, besides SPs, localized waveguide resonances or localized modes also make contributions to the extraordinary transmission of light in periodic subwavelength holes [29–31]. To better understand the transmission enhancement mechanism in the terahertz regime, we studied hole width-dependent terahertz transmission. A characteristic evolution, including well-regulated change in transmittance, linewidth broadening, and blueshift of peak transmission frequencies with respect to hole width, is experimentally observed [22]. Based on numerical analysis by the Fano model, we found that terahertz transmissions in the 2D hole arrays are associated with two types of contributions: resonant excitation of SPs and nonresonant transmission (or non-SP transmission). The nonresonant transmission exhibits angle-independent peak frequencies and can be resulted from localized effects and direct transmission [22, 23, 29–33]. The localized effects, as either localized modes or localized waveguide resonances [29–31], also contribute substantially to enhanced terahertz transmission. The direct transmission, on the other hand, due to scattering and low filling fraction of metal, is the origin that causes the reduction in transmission efficiency of the holes.

A set of 2D hexagonal arrays of rectangular subwavelength holes are lithographically fabricated with 180-nm-thick Al film onto a silicon wafer (0.64-mm-thick, p-type resistivity 20 Ωcm) [22]. Each sample, with dimensions of 15 × 15 mm^2, has holes of a fixed length 120 μm and various widths from 40 to 140 μm with a 20 μm interval and a constant lattice period of 160 μm. Figure 7 illustrates the frequency-dependent absolute transmittance and the corresponding phase change for an array with hole dimensions of 120 × 40 μm^2. At normal incidence, the resonant frequency can be approximately given by (1) with $G_{mn} = 4\pi(m^2 + n^2 + mn)^{1/2}/\sqrt{3}L$, the grating momentum wave vector for the 2D hexagonal hole arrays. The calculated fundamental SP [±1,0] resonance of hexagonal arrays at the Al-Si interface is around 0.63 THz, which is higher than the measured transmission peak 0.49 THz; the latter is a result of both resonant and nonresonant contributions [4, 12, 34].

The transmittance can be analyzed by the Fano model that involves two types of scattering processes: one refers to the continuum direct scattering state as nonresonant transmission, and the other is the discrete resonant state as SPs [23, 34–38]. For an isolated resonance, the Fano model can be written as $T_{\text{fano}}(\omega) = |t(\omega)|^2 = T_a + T_b(\varepsilon_\nu + q_\nu)^2/(1 + \varepsilon_\nu^2)$, where $\varepsilon_\nu = (\omega - \omega_\nu)/(\Gamma_\nu/2)$, T_a is a slowly varying transmittance, and $|T_b|$ is the contribution of a zero-order continuum state that couples with the discrete resonant state. The resonant state is characterized by the resonance frequency ω_ν, the linewidth Γ_ν, and the Breit-Wigner-Fano coupling coefficient q_ν [23, 34–38]. The Fano model provided a consistent fit to the measured transmittance as shown in Figure 7(a), with a peak transmission at $\omega_\nu/2\pi$ = 0.49 THz and a linewidth $\Gamma_\nu/2\pi$ = 0.16 THz.

The measured transmittance of the arrays with various hole widths from 40 to 140 μm shown in Figure 8(a) reveals a hole width dependent evolution. An optimal hole width exists (here, is 80 μm), with which the peak absolute transmittance T_P approaches the maximum value as depicted in Figure 8(b). Meanwhile, the resonance frequency and the corresponding linewidth exhibit monotonic changes. The all-out transmission probability can be obtained by solving the Hamiltonian $\hat{H} = \hat{H}_{\text{SP}} + \hat{H}_{\text{NRT}} + \hat{H}_{\text{Coupling}}$. Hence the coupling can be evaluated by diagonalizing the Hamiltonian matrix [13, 34, 35]

$$H = \hbar \begin{pmatrix} \omega_{\text{SP}} & \chi \\ \chi^* & \omega_{\text{NRT}} \end{pmatrix}, \tag{2}$$

where ω_{SP} is the resonance frequency of the SP mode given based on the momentum relationship, ω_{NRT} is the frequency of nonresonant transmission, and χ is the coupling coefficient between SPs and nonresonant transmission. Based on the angle-dependent transmission measurements for each array of different hole widths, the coupling $|\chi|^2$ at each angle of incidence can be solved [22].

Figure 9 shows the calculated coupling strength between the SP mode and nonresonant transmission for arrays with different hole widths at normal incidence. With increasing hole width, the coupling strength shows monotonic change; it is enhanced from $|\chi|^2 = 1.22 \times 10^{-3}$ at 40 μm to $|\chi|^2 = 6.21 \times 10^{-3}$ at 140 μm. This further explains the measured characteristic evolution in the transmission spectra of these arrays. The increase in hole width, that corresponds to

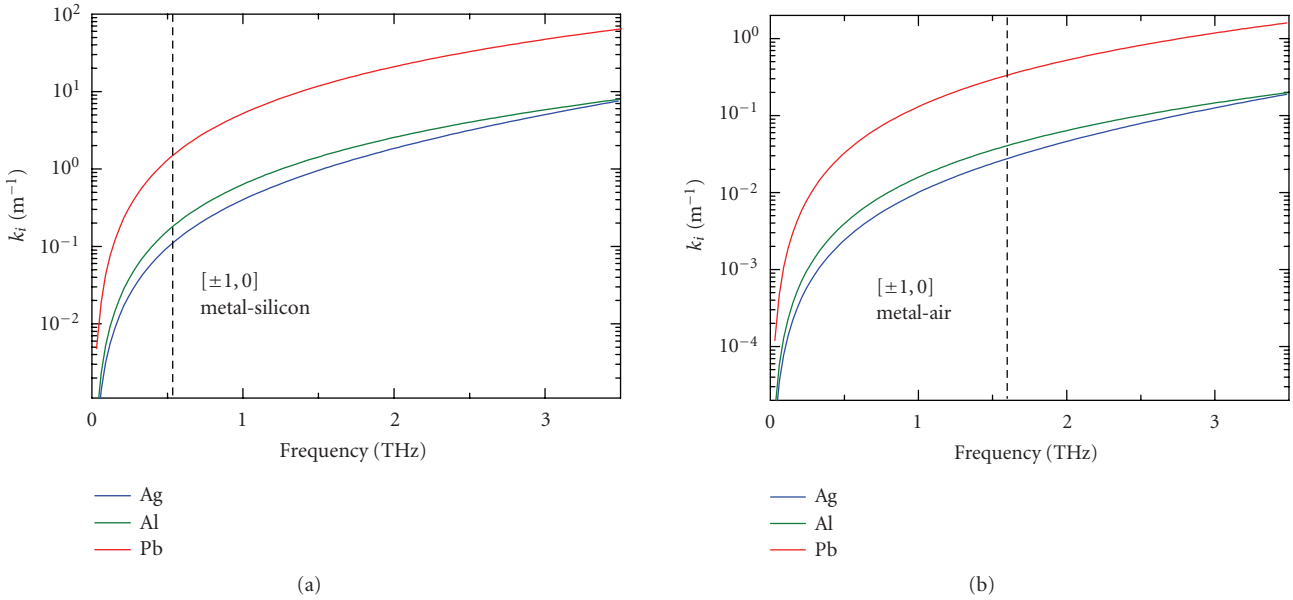

Figure 6: Frequency-dependent imaginary propagation vectors of SPs for Ag, Al, and Pb along (a) metal-Si interface and (b) metal-air interfaces.

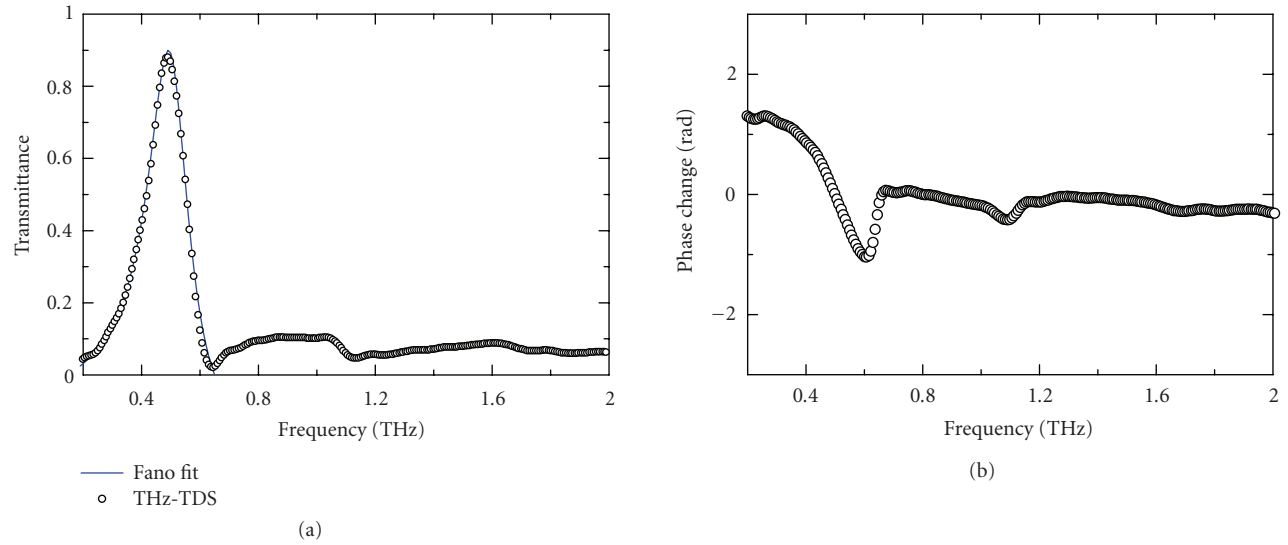

Figure 7: (a) Measured (open circles) and theoretical fit (solid curve) by the Fano model of frequency-dependent transmittance of the hexagonal array of 120 × 40 μm^2 holes. The fitting parameters are $q_v = 26.5 \pm 0.2$, $\omega_v/2\pi = 0.49 \pm 0.05$ THz, $\Gamma_v/2\pi = 0.16 \pm 0.01$ THz, and $T_b = (1.28 \pm 0.1) \times 10^{-3}$ for the [±1,0] mode. (b) Corresponding data of phase change.

reduced aspect ratio of holes and lower filling fraction of metal not only leads to increased direct transmission through the holes, but also enhances the coupling between SPs and nonresonant transmission. This, in turn, gives rise to an increased damping of SPs, and thus the linewidth broadens and shifts to higher frequencies towards the peak of nonresonant transmission [23, 29, 32–34]. Another evidence of the effect of direct transmission due to increased hole width is that, when the peak absolute transmittance T_P is normalized by the area of the holes as shown by the circles in Figure 8(b), it exhibits monotonic decrease with increasing hole width.

The maximum absolute peak transmittance T_P achieved at hole width 80 μm (aspect ratio 3 : 2, filling fraction of metal 62.5%) indicates that the negative effect of direct transmission becomes critical and challenges the dominant role of SPs and localized effects when the hole width is further increased. The contributions of localized effects and direct transmission to the effect of nonresonant terahertz transmission may vary with various hole width (or aspect ratio) and filling fraction of metal. For arrays with filling fraction of metal less than 80%, direct transmission contributes substantially to nonresonant transmission and causes the normalized transition efficiency declined monotonically.

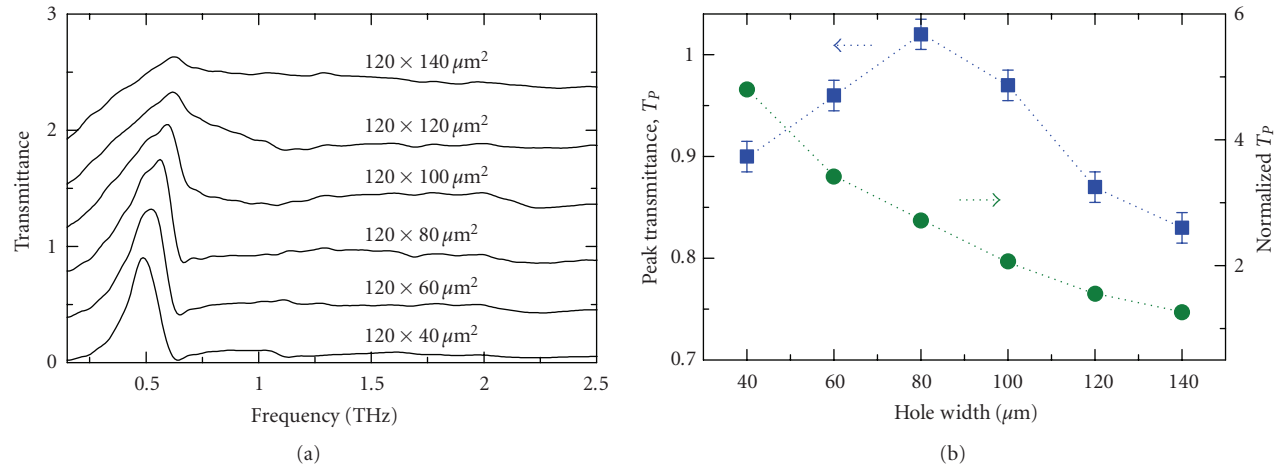

FIGURE 8: (a) Measured absolute transmittance of the hole arrays with fixed hole length of 120 μm and various hole widths from 40 to 140 μm. For clarity, the curves are vertically displaced by 0.36. (b) Absolute (squares) and normalized (circles) peak transmittance as a function of hole width. The dotted lines are a guide to the eye.

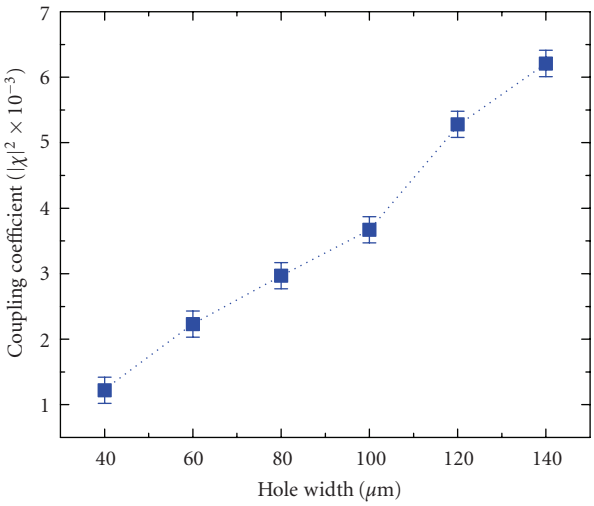

FIGURE 9: Calculated coupling coefficient of the Al-Si SP [±1,0] modes with nonresonant transmission for different hole widths at normal incidence. The dotted line is a guide to the eye.

3. CONCLUSION

In conclusion, transmission properties of terahertz pulses through 2D array of subwavelength metal holes were experimentally investigated. Conventional photolithographic process was used to pattern the subwavelength arrays on good and poor metallic conductors. Extraordinary terahertz transmission in such arrays was characterized by broadband THz-TDS measurements. The frequency-dependent resonant transmission in the 2D hole arrays is understood as a consequence of the resonance excitation of SPs at the metal-dielectric interface. We demonstrated the effect of hole shape, hole dimensions, dielectric properties of the metals, polarization dependence, and metal thickness on enhanced terahertz transmission. Rectangular hole shapes were found to show higher resonant transmission when the polarization of the incident terahertz field is perpendicular to the longer axis of the holes. Efficiently enhanced transmission was also observed in optically thin metallic arrays having thickness of one-third of the skin depth. For similar array transmission is higher for the array made from metal having higher electrical conductivity. In addition, the enhanced terahertz transmission in the 2D hole arrays is demonstrated as a result of contributions from both SPs and nonresonant transmission.

ACKNOWLEDGMENTS

The authors thank D. Qu, D. Grischkowsky, Y. Zhao, M. He, X. Lu, M. Gong, and J. Dai for their outstanding contributions and efforts in this work. This work was partially supported by the National Science Foundation.

REFERENCES

[1] T. W. Ebbesen, H. J. Lezec, H. F. Ghaemi, T. Thio, and P. A. Wolff, "Extraordinary optical transmission through subwavelength hole arrays," *Nature*, vol. 391, no. 6668, pp. 667–669, 1998.

[2] W. L. Barnes, A. Dereux, and T. W. Ebbesen, "Surface plasmon subwavelength optics," *Nature*, vol. 424, no. 6950, pp. 824–830, 2003.

[3] R. Gordon, A. G. Brolo, A. McKinnon, A. Rajora, B. Leathem, and K. L. Kavanagh, "Strong polarization in the optical transmission through elliptical nanohole arrays," *Physical Review Letters*, vol. 92, no. 3, Article ID 037401, 4 pages, 2004.

[4] D. Qu, D. Grischkowsky, and W. Zhang, "Terahertz transmission properties of thin, subwavelength metallic hole arrays," *Optics Letters*, vol. 29, no. 8, pp. 896–898, 2004.

[5] C. Janke, J. Gómez Rivas, C. Schotsch, L. Beckmann, P. Haring Bolivar, and H. Kurz, "Optimization of enhanced terahertz transmission through arrays of subwavelength apertures," *Physical Review B*, vol. 69, no. 20, Article ID 205314, 5 pages, 2004.

[6] H. Cao and A. Nahata, "Resonantly enhanced transmission of terahertz radiation through a periodic array of subwavelength apertures," *Optics Express*, vol. 12, no. 6, pp. 1004–1010, 2004.

[7] F. Miyamaru and M. Hangyo, "Finite size effect of transmission property for metal hole arrays in subterahertz region," *Applied Physics Letters*, vol. 84, no. 15, pp. 2742–2744, 2004.

[8] J. F. O'Hara, R. D. Averitt, and A. J. Taylor, "Terahertz surface plasmon polariton coupling on metallic gratings," *Optics Express*, vol. 12, no. 25, pp. 6397–6402, 2004.

[9] D. Qu and D. Grischkowsky, "Observation of a new type of THz resonance of surface plasmons propagating on metal-film hole arrays," *Physical Review Letters*, vol. 93, no. 19, Article ID 196804, 4 pages, 2004.

[10] A. K. Azad, Y. Zhao, and W. Zhang, "Transmission properties of terahertz pulses through an ultrathin subwavelength silicon hole array," *Applied Physics Letters*, vol. 86, no. 14, Article ID 141102, 3 pages, 2005.

[11] Q. Xing, S. Li, Z. Tian, et al., "Enhanced zero-order transmission of terahertz radiation pulses through very deep metallic gratings with subwavelength slits," *Applied Physics Letters*, vol. 89, no. 4, Article ID 041107, 3 pages, 2006.

[12] G. Torosyan, C. Rau, B. Pradarutti, and R. Beigang, "Generation and propagation of surface plasmons in periodic metallic structures," *Applied Physics Letters*, vol. 85, no. 16, pp. 3372–3374, 2004.

[13] J.-B. Masson and G. Gallot, "Coupling between surface plasmons in subwavelength hole arrays," *Physical Review B*, vol. 73, no. 12, Article ID 121401, 4 pages, 2006.

[14] A. K. Azad and W. Zhang, "Resonant terahertz transmission in subwavelength metallic hole arrays of sub-skin-depth thickness," *Optics Letters*, vol. 30, no. 21, pp. 2945–2947, 2005.

[15] A. K. Azad, M. He, Y. Zhao, and W. Zhang, "Effect of dielectric properties of metals on terahertz transmission subwavelength hole arrays," *Optics Letters*, vol. 31, no. 17, pp. 2637–2639, 2006.

[16] E. Ozbay, "Plasmonics: merging photonics and electronics at nanoscale dimensions," *Science*, vol. 311, no. 5758, pp. 189–193, 2006.

[17] H. Raether, *Surface Plasmons on Smooth and Rough Surfaces and on Gratings*, chapter 2, Springer, Berlin, Germany, 1988.

[18] W. Srituravanich, N. Fang, C. Sun, Q. Luo, and X. Zhang, "Plasmonic nanolithography," *Nano Letters*, vol. 4, no. 6, pp. 1085–1088, 2004.

[19] X. Luo and T. Ishihara, "Surface plasmon resonant interference nanolithography technique," *Applied Physics Letters*, vol. 84, no. 23, pp. 4780–4782, 2004.

[20] Z.-W. Liu, Q.-H. Wei, and X. Zhang, "Surface plasmon interference nanolithography," *Nano Letters*, vol. 5, no. 5, pp. 957–961, 2005.

[21] A. V. Zayats, J. Elliott, I. I. Smolyaninov, and C. C. Davis, "Imaging with short-wavelength surface plasmon polaritons," *Applied Physics Letters*, vol. 86, no. 15, Article ID 151114, 3 pages, 2005.

[22] J. Han, A. K. Azad, M. Gong, X. Lu, and W. Zhang, "Coupling between surface plasmons and nonresonant transmission in subwavelength holes at terahertz frequencies," *Applied Physics Letters*, vol. 91, no. 7, Article ID 071122, 3 pages, 2007.

[23] W. Zhang, A. K. Azad, J. Han, J. Xu, J. Chen, and X.-C. Zhang, "Direct observation of a transition of a surface plasmon resonance from a photonic crystal effect," *Physical Review Letters*, vol. 98, no. 18, Article ID 183901, 4 pages, 2007.

[24] T. Thio, H. F. Ghaemi, H. J. Lezec, P. A. Wolff, and T. W. Ebbesen, "Surface-plasmon-enhanced transmission through hole arrays in Cr films," *Journal of the Optical Society of America B*, vol. 16, no. 10, pp. 1743–1748, 1999.

[25] D. E. Grupp, H. J. Lezec, T. W. Ebbesen, K. M. Pellerin, and T. Thio, "Crucial role of metal surface in enhanced transmission through subwavelength apertures," *Applied Physics Letters*, vol. 77, no. 11, pp. 1569–1571, 2000.

[26] M. A. Ordal, L. L. Long, R. J. Bell, et al., "Optical properties of the metals Al, Co, Cu, Au, Fe, Pb, Ni, Pd, Pt, Ag, Ti, and W in the infrared and far infrared," *Applied Optics*, vol. 22, no. 7, pp. 1099–1119, 1983.

[27] L. Martín-Moreno, F. J. García-Vidal, H. J. Lezec, A. Degiron, and T. W. Ebbesen, "Theory of highly directional emission from a single subwavelength aperture surrounded by surface corrugations," *Physical Review Letters*, vol. 90, no. 16, Article ID 167401, 4 pages, 2003.

[28] H. J. Lezec and T. Thio, "Diffracted evanescent wave model for enhanced and suppressed optical transmission through subwavelength hole arrays," *Optics Express*, vol. 12, no. 16, pp. 3629–3651, 2004.

[29] K. L. van der Molen, K. J. Klein Koerkamp, S. Enoch, F. B. Segerink, N. F. van Hulst, and L. Kuipers, "Role of shape and localized resonances in extraordinary transmission through periodic arrays of subwavelength holes: experiment and theory," *Physical Review B*, vol. 72, no. 4, Article ID 045421, 9 pages, 2005.

[30] Z. Ruan and M. Qiu, "Enhanced transmission through periodic arrays of subwavelength holes: the role of localized waveguide resonances," *Physical Review Letters*, vol. 96, no. 23, Article ID 233901, 4 pages, 2006.

[31] A. Degiron and T. W. Ebbesen, "The role of localized surface plasmon modes in the enhanced transmission of periodic subwavelength apertures," *Journal of Optics A*, vol. 7, no. 2, pp. S90–S96, 2005.

[32] T. Matsui, A. Agrawal, A. Nahata, and Z. V. Vardeny, "Transmission resonances through aperiodic arrays of subwavelength apertures," *Nature*, vol. 446, no. 7135, pp. 517–521, 2007.

[33] F. J. García de Abajo, J. Sáenz, I. Campillo, and J. Dolado, "Site and lattice resonances in metallic hole arrays," *Optics Express*, vol. 14, no. 1, pp. 7–18, 2006.

[34] W. Fan, S. Zhang, B. Minhas, K. J. Malloy, and S. R. J. Brueck, "Enhanced infrared transmission through subwavelength coaxial metallic arrays," *Physical Review Letters*, vol. 94, no. 3, Article ID 033902, 4 pages, 2005.

[35] C. Genet, M. P. van Exter, and J. P. Woerdman, "Fano-type interpretation of red shifts and red tails in hole array transmission spectra," *Optics Communications*, vol. 225, no. 4–6, pp. 331–336, 2003.

[36] U. Fano, "Effects of configuration interaction on intensities and phase shifts," *Physical Review*, vol. 124, no. 6, pp. 1866–1878, 1961.

[37] M. Sarrazin, J.-P. Vigneron, and J.-M. Vigoureux, "Role of Wood anomalies in optical properties of thin metallic films with a bidimensional array of subwavelength holes," *Physical Review B*, vol. 67, no. 8, Article ID 085415, 8 pages, 2003.

[38] S.-H. Chang, S. K. Gray, and G. C. Schatz, "Surface plasmon generation and light transmission by isolated nanoholes and arrays of nanoholes in thin metal films," *Optics Express*, vol. 13, no. 8, pp. 3150–3165, 2005.